

2-1-2001

Charge exchange contribution to the decay of the ring current, measured by energetic neutral atoms (ENAs)

A. M. Jorgensen

M. G. Henderson

E. C. Roelof

G. D. Reeves

Harlan E. Spence

Boston University, harlan.spence@unh.edu

Follow this and additional works at: http://scholars.unh.edu/physics_facpub



Part of the [Physics Commons](#)

Recommended Citation

Jorgensen, A. M., M. G. Henderson, E. C. Roelof, G. D. Reeves, and H. E. Spence (2001), Charge exchange contribution to the decay of the ring current, measured by energetic neutral atoms (ENAs), *J. Geophys. Res.*, 106(A2), 1931–1937, doi:10.1029/2000JA000124.

This Article is brought to you for free and open access by the Physics at University of New Hampshire Scholars' Repository. It has been accepted for inclusion in Physics Scholarship by an authorized administrator of University of New Hampshire Scholars' Repository. For more information, please contact nicole.hentz@unh.edu.

Charge exchange contribution to the decay of the ring current, measured by energetic neutral atoms (ENAs)

Rights

Copyright 2001 by the American Geophysical Union.

Charge exchange contribution to the decay of the ring current, measured by energetic neutral atoms (ENAs)

A. M. Jorgensen,¹ M. G. Henderson,¹ E. C. Roelof,² G. D. Reeves,¹ and H. E. Spence³

Abstract. In this paper we calculate the contribution of charge exchange to the decay of the ring current. Past works have suggested that charge exchange of ring current protons is primarily responsible for the decay of the ring current during the late recovery phase, but there is still much debate about the fast decay of the early recovery phase. We use energetic neutral atom (ENA) measurements from Polar to calculate the total ENA energy escape. To get the total ENA escape we apply a forward modeling technique, and to estimate the total ring current energy escape we use the Dessler-Parker-Sckopke relationship. We find that during the late recovery phase of the March 10, 1998 storm ENAs with energies greater than 17.5 keV can account for 75% of the estimated energy loss from the ring current. During the fast recovery the measured ENAs can only account for a small portion of the total energy loss. We also find that the lifetime of the trapped ions is significantly shorter during the fast recovery phase than during the late recovery phase, suggesting that different processes are operating during the two phases.

1. Introduction

In this paper we calculate the contribution of charge exchange to the decay of the ring current. We do this through the analysis of measurements of energetic neutral atoms (ENAs), which are the direct product of the charge exchange reaction.

The mechanisms responsible for the decay of the storm time ring current are still a matter of debate. *Hamilton et al.* [1988] suggested, based on AMPTE/CCE measurements, that the initial rapid decay of the ring current was due to charge exchange of O^+ , while the slower decay was due to charge exchange of H^+ . *Daglis* [1997] obtained similar results. However, recent modeling results have not been able to confirm this. *Jordanova et al.* [1996, 1998] have shown that charge exchange is the most important collisional loss mechanism, but not necessarily that it is the most important loss process. Using time-dependent convection models, *Fok et al.* [1995] and *Kozyra et al.* [1998] found that in addition to charge exchange loss, convection loss through the dayside magnetopause, and Coulomb collision loss, other loss processes must be operating. *Liemohn et al.* [1999] demonstrated that the convective loss through the dayside magnetopause is dominant.

Moritz [1972] and *Mizera and Blake* [1973] first suggested that low-altitude particle populations originated from the ring current through charge exchange, but the first direct measurements of ENAs were reported by *Hovestadt and Scholer* [1976]. *Roelof et al.* [1985] analyzed complete storms and were able to associate the ENA flux measured with the decay rate of the ring current, concluding that the ENA emission was roughly equal to the energy loss from the ring current. Most recently, *Jorgensen et al.* [1997] showed that the ENA count rate from the Polar satellite, when corrected for orbital motion, exhibited a rough proportionality with the *Dst* index, not only for single storms, but over long time periods. This result prompted *Ebihara et al.* [1999] to undertake a theoretical simulation. They found that for relatively low energies (below approximately 150 keV), there was indeed a proportionality between *Dst* and ENA flux. In addition, the asymmetries of the magnetic field could cause single injections to exhibit oscillatory ENA production as the injected particles travel around the Earth.

In this paper we will calculate the total charge exchange energy escape rate out of the ring current using direct measurements of ENAs. Because the ENAs are the product of charge exchange, the calculation of the charge exchange contribution can be performed directly, unlike past estimates, which could only be inferred from the in situ measurements of ring current ions.

2. Theory

In order to calculate the charge exchange contribution to the energy loss from the ring current, we need to be able to calculate the total energy carried out of the ring

¹Los Alamos National Laboratory, Los Alamos, New Mexico.

²The Johns Hopkins University Applied Physics Laboratory, Laurel, Maryland.

³Center for Space Physics, Boston University, Boston, Massachusetts.

current due to ENAs, dE_{ENA}/dt , and the total energy loss from the ring current, dW_P/dt .

The total ENA energy escape is simply the integral over energy, solid angle, and space of the unidirectional ENA production rate,

$$\frac{dE_{ENA}}{dt} = \int dE E \int d^3r \int d^2\Omega \frac{d^5n}{d^3r d^2\Omega dE dt}, \quad (1)$$

and the unidirectional differential ENA production rate is

$$\frac{d^5n}{d^3r d^2\Omega dE dt} = \sigma n_H j_{ION}, \quad (2)$$

where σ is the charge exchange cross section, n_H is the geocoronal neutral density, and j_{ION} is the ion flux. The units of the left-hand side are thus $(\text{cm}^3 \text{sr keV s})^{-1}$. Thus by substitution, the ENA energy escape rate is simply

$$\frac{dE_{ENA}}{dt} = \int dE E \int d^3r \int d^2\Omega \sigma n_H j_{ION}. \quad (3)$$

An important point to notice here is that the integral is over the product $\sigma n_H j_{ION}$. This means that the resulting computation of the energy escape depends not on correct specification of the absolute magnitude of σ , n_H , and j_{ION} separately, but only on the specification of the absolute magnitude of the product. The radial shape of the neutral density is much better known than its absolute value at any given time. This point will be elaborated on in section 4.

To estimate the total energy loss from the ring current, we will use the Dessler-Parker-Sckopke (DPS) relation [Dessler and Parker, 1959; Sckopke, 1966], which is a method for estimating the total energy of ring current particles. The DPS relation,

$$\frac{\Delta B}{B_0} = -\frac{2 W_P}{3 W_M}, \quad (4)$$

presents a relationship between the energy of particles (W_P) in a magnetic dipole field with energy W_M , and the relative magnetic disturbance created at the location of the magnetic dipole. B_0 is the magnetic field measured at a given radial location R_0 in the dipole equator, and W_M is integrated outside that radial distance. Thus for the Earth, typically B_0 is considered the magnetic field at the dipole equator on the surface of the Earth, while W_M is the energy of the portion of the field that is outside the Earth. This expression is derived for nonconducting conditions. If there is a uniformly conducting sphere at the origin with radius R_0 , then a multiplicative factor greater than 1, and no greater than 1.5, must be included on the right-hand side of equation (4). In this paper we assume a perfectly conducting Earth, which corresponds to a multiplicative factor of 1.5, so that the DPS relation becomes

$$\frac{\Delta B}{B_0} = -\frac{W_P}{W_M}. \quad (5)$$

Since ΔB cannot be measured, an often used approximation is Dst^* , which is the Dst index corrected for solar wind dynamic pressure [Burton et al., 1975; McPherron, 1997],

$$Dst^* = Dst - b\sqrt{p} + c, \quad (6)$$

where $b = 0.2 \text{ nT}\sqrt{\text{eV}/\text{cm}^3}$, and $c = 20 \text{ nT}$. The estimated total energy in the ring current is thus

$$W_P = -\frac{Dst^*}{B_0} W_M, \quad (7)$$

and the total estimated energy escape rate out of the ring current is

$$\frac{dW_P}{dt} = -\frac{dDst^*}{dt} W_M. \quad (8)$$

We are thus interested in measuring how much of dW_P/dt (equation (8)) can be accounted for with dE_{ENA}/dt (equation (3)).

It should be mentioned in this context that there is still much debate regarding the connection between the ring current and the Dst index. The debate focuses primarily on whether Dst is solely or mostly due to the ring current [i.e., Kamide et al., 1998; Greenspan and Hamilton, 2000; Turner et al., 2000, also A. M. Jorgensen et al., A statistical study of the global structure of the ring current, submitted to *Journal of Geophysical Research*, 2000]. In this paper we implicitly assume that Dst^* (as calculated from equation (6)) is entirely due to the ring current.

3. Data Set

For this study we use the Polar Comprehensive Energetic Particle and Pitch Angle/Imaging Proton Spectrometer (CEPPAD/IPS) data set. The instrument has nine look directions and uses the spin of the spacecraft to sample the complete unit sphere in up to 288 pixels. See, for example, Figure 1 and Figure 2c of Henderson et al. [1997] for an illustration of the viewing geometry. For a complete description of the instrument, see Blake et al. [1995]. The instrument measures ions and neutrals with energies between 17.5 keV and 1500 keV. The instrument is not capable of distinguishing between ENAs and ions. However, the distinction can be inferred from the pitch angle distribution. ENAs tend to be a relatively weak signal arriving from the Earth direction and show no symmetry with respect to the magnetic field. When Polar passes through the polar caps where the energetic ion fluxes are very low, these weak directional ENA signals become clear. Polar spends approximately half its time in the polar caps, thus providing a 50% duty cycle with a repeat period of 18 hours.

For this paper we analyze the March 10, 1998 storm. The Dst time series for the March 10, 1998, storm is

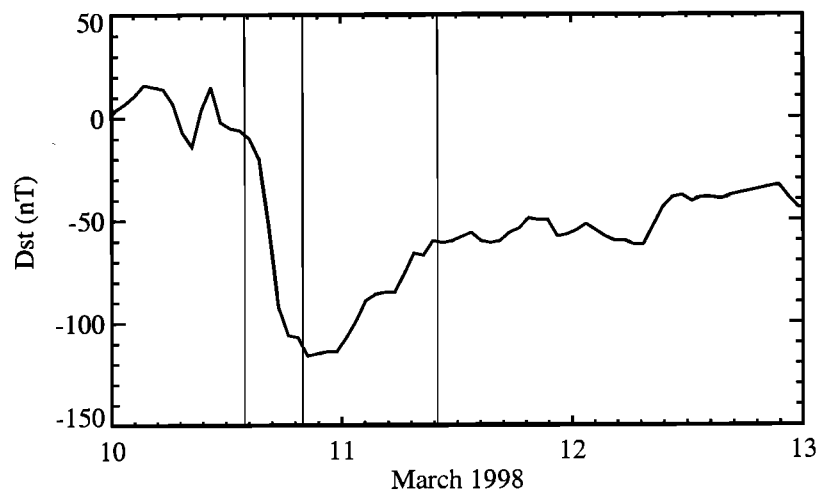


Figure 1. *Dst* index for the March 10, 1998, magnetic storm. The three vertical lines mark the beginning of the main phase, fast recovery phase, and slow recovery phase.

shown in Figure 1. During the time interval March 10, 1998, 0000 UT, to March 13, 1998, at 0000 UT, we computed cleaned ENA images on the hour whenever Polar was in the polar caps.

The cleaning procedure involves removing non-ENA contamination in the images. There are two types of contamination: sunlight and earthlight response, and a uniform background count rate due to low levels of ions in the polar caps, as well as electronic noise in the instrument. We start with the 96-s average data sets. These data are manually checked for sunlight and earthlight contamination, and contaminated pixels are marked as bad. Next the ion and noise background was subtracted. The noise was computed separately for each of the nine look directions as the median count rate in that look direction. Then the noise was subtracted, and counting uncertainty on each pixel was computed.

Finally, 15 min worth of 96-s average images were averaged together, and the counting uncertainty was carried through the addition. The resulting data set consisted of 34 time intervals, sampled in seven energy bins (17.5–22.6 keV, 22.6–30.3 keV, 30.3–41.4 keV, 41.4–55.9 keV, 55.9–75.9 keV, 79.5–103 keV, and 103–142 keV), for a total of 238 images. We do not show images in this paper, but several sample images were given by *Henderson et al.* [1997, 1999]

4. Analysis

The first step in the analysis is to extract the ENA source function (equation (2)). We wish to determine at every point in space the production rate of ENAs. The ENA source function is the product of the ion flux j_{ION} , the neutral density n_H , and the charge exchange cross section σ . We use a fixed model for n_H , a constant for σ , and a parameterized model for the ion flux. This extraction method has been described in detail by *Henderson et al.* [1999] and *Roelof* [1987]. It is a forward

modeling approach, in which parameters to a model are varied until an ENA image simulated from the model matches sufficiently well with the measured ENA image.

We used a modification of the 10-parameter model presented by *Roelof et al.* [1992, 1993] and *Chase and Roelof* [1995]. The modifications consisted of fixing four of the parameters: $dL_1 = 0.333$, $dL_2 = 1.0$, $k_2 = 0$, and $\phi_2 = 0$, thereby effectively creating a six-parameter model. We used the model of *Rairden et al.* [1986] as the neutral atmosphere model. We used an efficient line minimization technique [*Brent*, 1973; *Lau*, 1995] to optimize the fits. See the description of *Henderson et al.* [1999] for more details.

For each of the 238 ENA images, the forward modeling procedure is applied. The result is six parameters for each image. The six parameters completely describe the function j_{ION} in equation (3) in each of the seven energy bins. For each of the seven energy bins, equation (3) is calculated using the same n_H and σ that were used to obtain the six model parameters. Finally, the ENA energy escape rate calculated for the seven channels is summed to yield the total ENA energy escape rate.

At this point we reiterate and expand on a statement from earlier. Since we use the same n_H in both the forward model and in the integration in equation (3), the absolute magnitude of n_H cancels out. In other words, we only need to know n_H to within a multiplicative constant in order to perform the calculation. This greatly improves the amount of trust we can put in the results, for the radial shape of the geocoronal density is known much better than its absolute magnitude. The latter varies daily with solar activity, while the former is controlled by processes that do not depend much on solar activity. Furthermore, because the forward modeling involves a division by the charge exchange cross section, σ , and the energy calculation involves multiplying by it, σ cancels out of the computation, and we

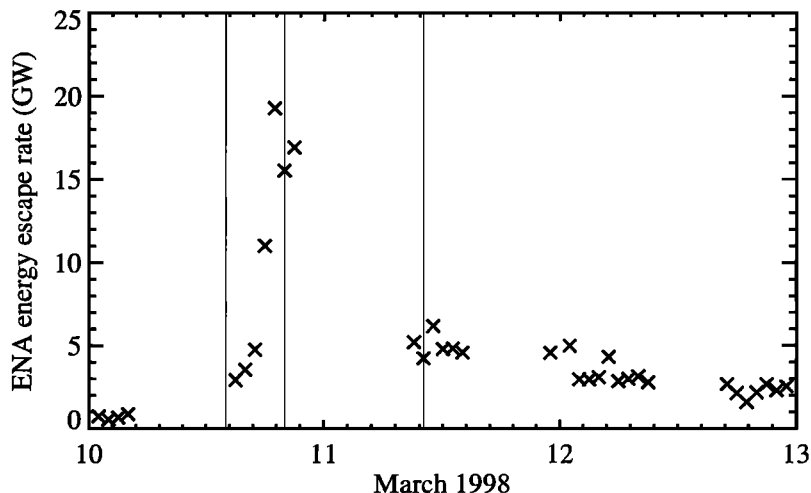


Figure 2. ENA energy escape rate for the March 10, 1998, storm.

can choose any values we want for σ . In essence we are using a procedure for extracting j_{ION} to extract the parameters for the product $\sigma n_H j_{ION}$. If we were ultimately interested in the values of j_{ION} separately, we would of course need to specify σn_H correctly.

The ENA energy escape rate is shown in Figure 2. These numbers are calculated under the assumption that all the measured ENAs are hydrogen. The instrument threshold to hydrogen is 17.5 keV, whereas its threshold to oxygen is approximately 60 keV. Because of the steep energy spectrum, the ENAs are dominated by particles near the lower threshold. This means that if all measured ENAs were oxygen instead of hydrogen, the calculated energies would have to be approximately doubled. However, in this paper we will concentrate on the late recovery phase, when high-energy oxygen is not expected.

Using equation (6) we can compute Dst^* (shown in Figure 3) from Dst (shown in Figure 1). We used the Wind/Solar Wind Experiment calculated dynamic pressure for this correction. Then, using equation (7) we

compute the estimated total ring current energy shown in Figure 4. Now, because of short-term fluctuations in the ring current energy, it is not convenient to simply take the derivative of it in order to obtain the ring current energy loss. Smoothing is also not feasible, since a window of at least 24 hours would be required to smooth the data sufficiently. This would severely distort the computed ring current energy loss rate. A better approach is to fit reasonable functional forms to the decay phase (the portion after the peak). We chose two functional forms to fit. One consisted of two exponentials,

$$E_{RC} = a_0 \exp\left(\frac{-(t-t_0)}{\tau_0}\right) + a_1 \exp\left(\frac{-(t-t_0)}{\tau_1}\right), \quad (9)$$

and the other consisted of a straight line plus an exponential,

$$E_{RC} = \max\left(a_0 - (t-t_0) \frac{a_0}{\tau_0}, 0\right) + a_1 \exp\left(\frac{-(t-t_0)}{\tau_1}\right), \quad (10)$$

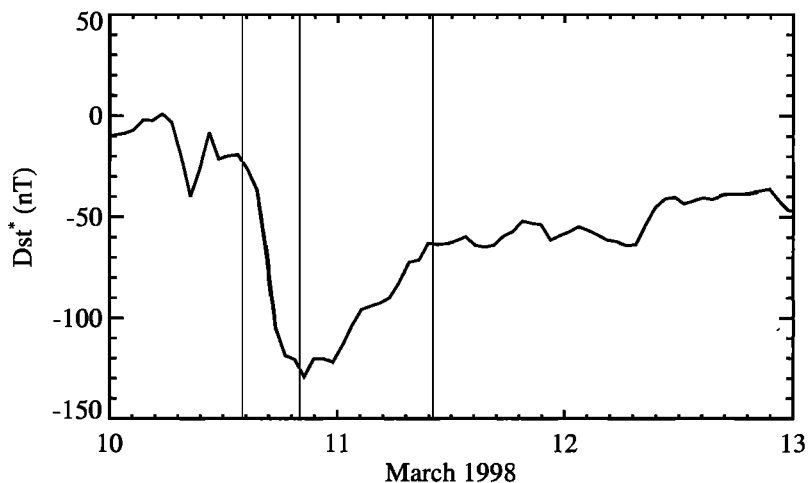


Figure 3. Dst^* for the March 10, 1998, storm.

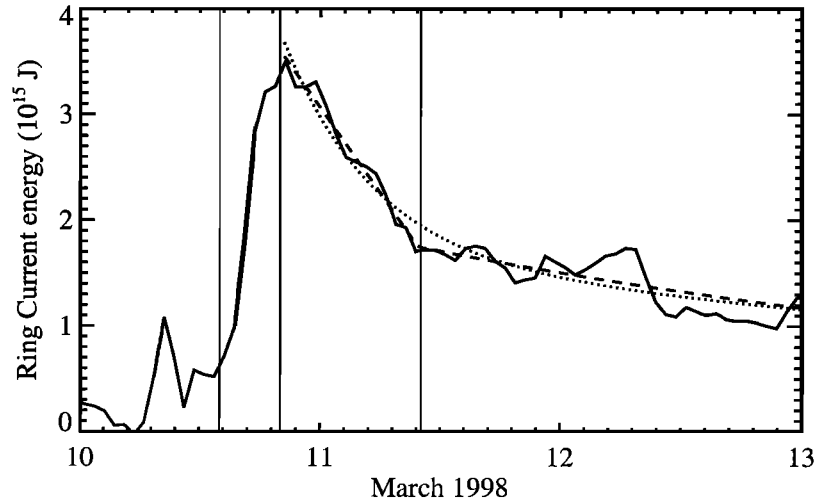


Figure 4. Estimated total ring current energy as derived from *Dst** (solid line), and fit of two exponentials (dotted line), and a straight line plus an exponential (dashed line) to the recovery phase.

with the straight line representing the fast decay. In Figure 4 the two exponentials are shown as a dotted line with parameters $[a_0, \tau_0, a_1, \tau_1] = [20.60 \times 10^{15} \text{J}, 0.363 \text{ days}, 1.97 \times 10^{15} \text{J}, 5.58 \text{ days}]$, while the straight line plus an exponential is shown as a dashed line with parameters $[a_0, \tau_0, a_1, \tau_1] = [3.90 \times 10^{15} \text{J}, 1.406 \text{ days}, 2.48 \times 10^{15} \text{J}, 4.01 \text{ days}]$. Time t_0 was chosen as 0000 UT on March 10, 1998.

Then, taking the time derivatives of equations (9) and (10), we obtain the estimated total ring current energy loss for these two models. It is plotted in Figure 5. We immediately notice that the two models yield quite different energy escape rates for the early recovery phase, but that they are consistent for the late decay. Finally, the measured ENA energy escape rate is plotted in Figure 5 as “+”-signs.

5. Results and Discussion

As we examine Figure 5, we can see that during the late decay of the storm, March 12, the measured ENAs can account for, on average, 75% of the estimated total energy loss from the ring current. The two fitted models of the ring current energy decay rate are also in close agreement during this time period. Our results are in good agreement with previous expectations for this phase of the storm [e.g., *Hamilton et al.*, 1988; *Daghs*, 1997], namely, that charge exchange of ring current protons dominates the late decay of the ring current. However, whereas these conclusions were indirectly arrived at in the past, the present results demonstrate the first direct measurements of the product of the charge exchange decay.

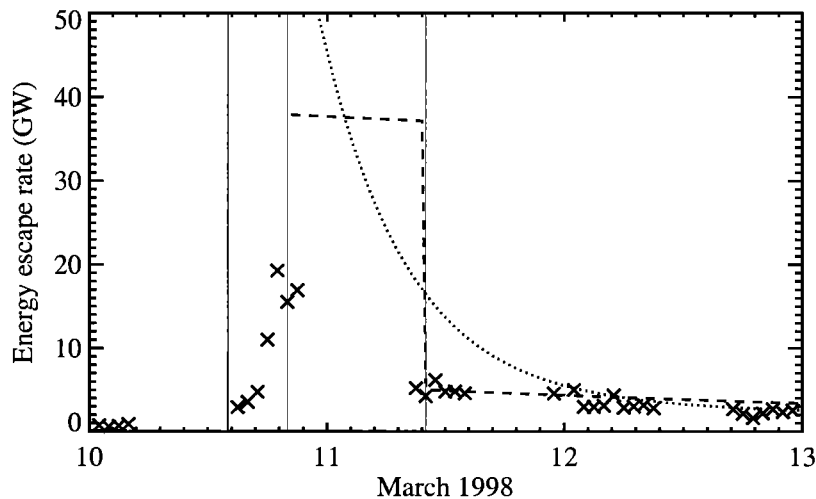


Figure 5. Energy escape rate out of the ring current, as measured by Polar (+), as calculated from two exponential fits (dotted line), and as calculated from a line plus an exponential fit (dashed line)

Next, let us examine the fast recovery. During this phase there was a data gap as the Polar satellite passed through the radiation belts where it is unable to measure ENAs. However, the measurements near the peak of the storm (late on March 11) can reasonably be taken as being indicative of the early fast recovery phase. However, there are two important points in this regard. First, we see that the two models in Figure 5 yield quite different energy loss rate time profiles during the fast recovery phase. However, if we examine Figure 4, they both appear to fit the ring current energy profile equally well. Therefore it is impossible to tell whether the energy loss is very rapid during the early fast recovery, and decreases later during the fast recovery, or whether it is nearly constant throughout the fast recovery phase. In either case, however, we find that the measured ENAs can only account for a small fraction of the ring current energy loss (Figure 5). This is, as mentioned earlier, under the assumption that all ENAs measured are hydrogen. If all the ENAs measured during the fast recovery are oxygen, then we would need to approximately double this figure. This would put the measured ENA energy escape in better agreement with the fitted models. However, it would require that the ring current oxygen is dominated by energies above 60 keV, which is an unlikely scenario. Therefore, at the present, there are still some ambiguities concerning the fast recovery mechanism. However, it is quite clear from the late decay measurements that the technique used works and provides an accurate measure of the ENA energy loss. In a future paper we will process different storms that yield a better picture of the fast decay.

Having now confirmed the source of the slow decay, it would be interesting to see if the ENA emissions during the fast decay are consistent with the same decay time (implying similar mechanisms and spectra) as the slow decay. *Jorgensen et al.* [1997] showed that there was a

rough proportionality between *Dst* and the count rate of ENAs with energy 17.5 keV. However, they also noted that near the peak of the storm and during the early recovery phase, there was a tendency for the ENA count rate to overshoot relative to *Dst*. We can examine this quantitatively. We know that during the late phase the decay time is 5.6 or 4.0 days, depending on which model we fit to the estimated ring current energy. If we thus divide the ring current energy in Figure 4 by this decay time, we obtain a predicted ENA energy escape rate, based on the same mechanism, spectrum, and species as during the slow recovery phase. This result is plotted in Figure 6. In this figure the dashed line represents a 4.0-day decay time, and the dotted line represents a 5.6-day decay time. We, of course, find that during the late decay phase there is good agreement between this model and the data, since we used data during this period to build the model. However, near the peak of the storm, we see that the measured ENA energy flux is 50-100% larger. What this means is that the decay time of the ENAs that we measure is two thirds to half of the decay time of the ENAs measured during the late decay phase. There can be several reasons for this, including different energy spectra, different spatial distributions, and different species.

6. Conclusion

We find that during the late, slow recovery phase of a magnetic storm, ENAs with energy above 17.5 keV can account for 75% of the estimated total energy loss from the ring current. While this has already been inferred indirectly by in situ ion measurements, our measurements present the first direct measurement of the product of the charge exchange reaction, thereby proving that charge exchange of protons dominates during that phase. During the fast recovery phase we find that

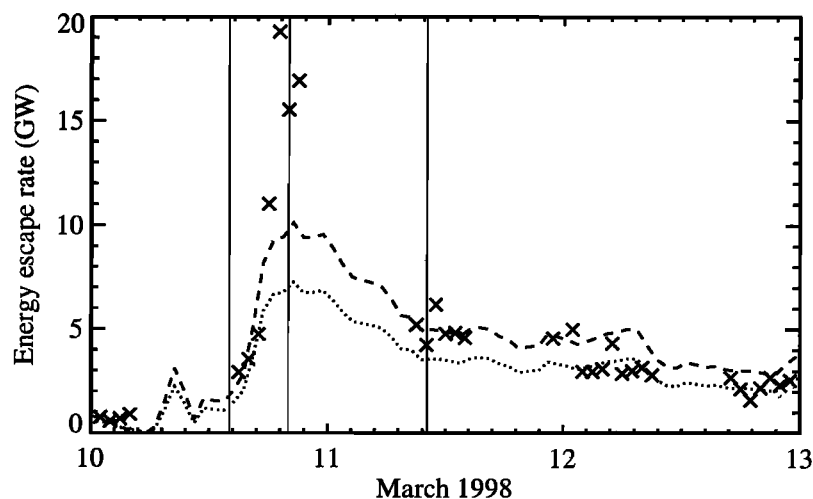


Figure 6. Predicted ring current energy loss from ENAs assuming same distribution as during the slow recovery phase, for all times. Shown are Polar-measured ENA escape rate (+), prediction using slow decay from two exponentials (dotted line), and prediction using slow decay from line plus an exponential (dashed line)

the measured ENAs can only account for a small fraction of the ring current energy loss, but also that the ENAs are emitted at a rate corresponding to a shorter lifetime than that of the late decay phase. In a future paper we will more closely examine the fast recovery and compare it to numerical models.

Acknowledgments. Work at Los Alamos National Laboratory was conducted partially under the auspices of the U. S. Department of Energy, with support from the NASA ISTP and SR&T programs. Work at Boston University was supported by NASA grants NAG5-7706 and NAG5-8039.

Janet G. Luhmann thanks Ioannis A. Daglis and another referee for their assistance in evaluating this paper.

References

- Blake, J. B., et al., CEPPAD: Comprehensive Energetic Particle and Pitch-Angle Distribution experiment on Polar, *Space Sci. Rev.*, **71**, 531, 1995.
- Brent, R. P., *Algorithms for Minimization Without Derivatives*, Prentice-Hall, Englewood Cliffs, N. J., 1973.
- Burton, R. K., R. L. McPherron, and C. T. Russell, Empirical relationship between interplanetary conditions and *Dst*, *J. Geophys. Res.*, **80**, 4204, 1975.
- Chase, C. J., and E. C. Roelof, Extracting evolving structures from global magnetospheric images via model fitting and video visualization, *Johns Hopkins APL Tech. Dig.*, **16**, 111, 1995.
- Daglis, I. A., The role of magnetosphere-ionosphere coupling in magnetic storm dynamics, in *Magnetic Storms*, edited by B. T. Tsurutani, W. D. Gonzalez, Y. Kamide, and J. K. Arballo, vol. 98 of *Geophys. Monogr. Ser.*, p. 107, AGU, Washington, D. C., 1997.
- Dessler, A. J., and E. N. Parker, Hydromagnetic theory of geomagnetic storms, *J. Geophys. Res.*, **64**, 2239, 1959.
- Ebihara, Y., S. Barabash, and M. Ejiri, On the global production rates of energetic neutral atoms (enas) and their association with the *Dst* index, *Geophys. Res. Lett.*, **26**, 2929, 1999.
- Fok, M.-C., T. E. Moore, J. U. Kozyra, G. C. Ho, and D. C. Hamilton, Three-dimensional ring current decay model, *J. Geophys. Res.*, **100**, 111, 1995.
- Greenspan, M. E., and D. C. Hamilton, A test of the Dessler-Parker-Sckopke relation during magnetic storms, *J. Geophys. Res.*, **105**, 5419, 2000.
- Hamilton, D. C., G. Gloeckler, F. M. Ipavich, W. Studemann, B. Wilken, and G. Kremser, Ring current development during the great magnetic storm of February 1986, *J. Geophys. Res.*, **93**, 14,343, 1988.
- Henderson, M. G., G. D. Reeves, H. E. Spence, R. B. Sheldon, A. M. Jorgensen, J. B. Blake, and J. F. Fennell, First energetic neutral atom images from Polar, *Geophys. Res. Lett.*, **24**, 1167, 1997.
- Henderson, M. G., G. D. Reeves, K. R. Moore, H. E. Spence, A. M. Jorgensen, J. F. Fennell, J. B. Blake, and E. C. Roelof, Energetic neutral atom imaging with the Polar CEPPAD/IPS instrument: Initial forward modeling results, *Phys. Chem. Earth, Part C, Solar Terr. and Planet. Sci.*, **24**(1-3), 203-208, 1999.
- Hovestadt, D., and M. Scholer, Radiation belt-produced energetic hydrogen in interplanetary space, *J. Geophys. Res.*, **81**, 5039, 1976.
- Jordanova, V. K., L. M. Kistler, J. U. Kozyra, G. V. Khazanov, and A. F. Nagy, Collisional loss of ring current ions, *J. Geophys. Res.*, **101**, 111, 1996.
- Jordanova, V. K., et al., October 1995 magnetic cloud and accompanying storm activity: Ring current evolution, *J. Geophys. Res.*, **103**, 79, 1998.
- Jorgensen, A. M., H. E. Spence, M. G. Henderson, G. D. Reeves, M. Sugiura, and T. Kamei, Global energetic neutral atom (ENA) measurements and their association with the *Dst* index, *Geophys. Res. Lett.*, **24**, 3173, 1997.
- Kamide, Y., et al., Current understanding of magnetic storms: Storm/substorm relationships, *J. Geophys. Res.*, **103**, 17,705, 1998.
- Kozyra, J. U., M.-C. Fok, E. R. Sanchez, D. S. Evans, D. C. Hamilton, and A. F. Nagy, The role of precipitation loss in producing the rapid early recovery phase of the great magnetic storm of February 1986, *J. Geophys. Res.*, **103**, 6801, 1998.
- Lau, H. T., *A Numerical Library in C for Scientists and Engineers*, CRC Press, Boca Raton, Fla., 1995.
- Liemohn, M. W., J. U. Kozyra, V. K. Jordanova, G. V. Khazanov, M. F. Thomsen, and T. E. Cayton, Analysis of early phase ring current recovery mechanisms during geomagnetic storms, *Geophys. Res. Lett.*, **26**, 2845, 1999.
- McPherron, R. L., The role of substorms in the generation of magnetic storms, in *Magnetic Storms*, edited by B. T. Tsurutani, W. D. Gonzalez, Y. Kamide, and J. K. Arballo, vol. 98 of *Geophys. Monogr. Ser.*, p. 117, AGU, Washington, D. C., 1997.
- Mizera, P. F., and J. B. Blake, Observations of ring current protons and low altitudes, *J. Geophys. Res.*, **78**, 1058, 1973.
- Moritz, J., Energetic protons and low equatorial altitudes, *Z. Geophys.*, **38**, 701, 1972.
- Rairden, R. L., L. A. Frank, and J. D. Craven, Geocoronal imaging with Dynamics Explorer, *J. Geophys. Res.*, **91**, 3613, 1986.
- Roelof, E. C., Energetic neutral atom imaging of a storm-time ring current, *Geophys. Res. Lett.*, **14**, 652, 1987.
- Roelof, E. C., D. G. Mitchell, and D. J. Williams, Energetic neutral atoms ($E > 50$ keV) from the ring current: IMP 7/8 and ISEE 1, *J. Geophys. Res.*, **90**, 10,991, 1985.
- Roelof, E. C., B. H. Mauk, R. R. Meier, and E. O. Hulbert, Instrument requirements for imaging the magnetosphere in extreme-ultraviolet and energetic neutral atoms derived from computer-simulated images, *Proc. SPIE Int. Soc. Opt. Eng.*, **1744**, 19, 1992.
- Roelof, E. C., B. H. Mauk, R. R. Meier, K. R. Moore, and R. A. Wolf, Simulations of EUV and ENA magnetospheric images based on the rice convection model, *Proc. SPIE Int. Soc. Opt. Eng.*, **2008**, 202, 1993.
- Skopke, N., A general relation between the energy of trapped particles and the disturbance field near the Earth, *J. Geophys. Res.*, **71**, 3125, 1966.
- Turner, N. E., D. N. Baker, T. I. Pulkkinen, and R. L. McPherron, Evaluation of the tail current contribution to *Dst*, *J. Geophys. Res.*, **105**, 5431, 2000.

M. G. Henderson, Los Alamos National Laboratory, Mail Stop D-436, SM-30, Bikini Atoll Road, Los Alamos, NM 87545. (mhenderson@lanl.gov)

A. M. Jorgensen and G. D. Reeves, Los Alamos National Laboratory, Mail Stop D-466, SM-30, Bikini Atoll Road, Los Alamos, NM 87545. (ajorg@lanl.gov; reeves@lanl.gov)

E. C. Roelof, The Johns Hopkins University/Applied Physics Laboratory, 11100 Johns Hopkins Road, Laurel, MD 20723-6099. (edmond.roelof@jhuapl.edu)

H. E. Spence, Center for Space Physics, Boston University, 725 Commonwealth Avenue, Boston, MA 02215. (spence@bu.edu)

(Received March 29, 2000; revised May 30, 2000; accepted June 26, 2000.)